Proposed Damage Control of Underground Infrastructure by Sheet Pile Construction at Liquefiable Urban Areas

Mohammad Reza OKHOVAT*, Shang FENG**, Koichi MAEKAWA***
Engineer, Division of Civil Engineering Design, Shimizu Corporation, Japan *
Research Fellow, Hydro Science and Engineering, Tsinghua University, P. R. China**
Professor, Department of Civil Engineering, The University of Tokyo, Japan***

ABSTRACT: The nonlinear seismic responses of underground RC ducts suspended in saturated liquefiable sandy deposit are investigated by simulating coupled soil-structure kinematics. The effect of sheet piling on both uplift and RC shear deterioration related to cracking of concrete and yield of steel is focused as a possible way of damage control of existing infrastructure. The uplift of underground structures is expected to be fairly confined by sheet piling of higher cost performance as investigated in the past researches. Concurrently, the amplified shear damage to RC ducts is newly found as a trade-off. But, its increased damage of RC ducts is estimated to be acceptable in view of urban infra-stock management in practice.

KEYWORDS: Stock management, Sheet pile, Liquefaction, Damage control, Underground structures

1. INTRODUCTION

Soil liquefaction is a typical phenomenon in soft alluvial deposits near coastline and/or river-mouth where most local governmental administration is being operated in Japan. Then, in view of the infra-stock management and urban safety, damage control of infrastructures with lower cost is an urgent issue. One of the stock damage is the rigid-body motion like uplift and floatation of underground space structures. The other is the structural destruction associated with cracking-crushing of concrete and yield of reinforcing steel, which is highly related to deformation during seismic events accompanying liquefaction.

The seismic undesirable events related to soil liquefaction were detected as early as in 1964 Niigata and Alaska earthquakes (Hall and O'Rourke 1991). Some troubles to pipelines or even large underground structures embedded in liquefiable soils were also found in the past earthquakes (Ishihara et al. 1993, Koseki et al. 1998 and Wang et al. 2001). Many researches have been performed and the uplift body motion has been focused. Koseki et al. (1994) carried out model shaking tests and successful finite element analysis to scrutinize the uplift of utility ducts.

Various preventive countermeasures have been studied and developed in practice to keep underground structures functional. Those can be basically classified into three categories; ground improvement, drainage of underground water and suppression of shear deformations. Amid these strategies, installation of sheet pile walls beside underground ducts or on-ground tanks is known to be effective in reducing both uplift and sinking-down, respectively (Kimura et al. 1995). Zheng et al. (1996) evaluated the efficiency of sheet pile-ring as a

countermeasure against liquefaction for oil tank sites, and concluded that the excess pore water pressure and the settlement of the tank could be significantly reduced by using a sheet pile-ring. In another view, some researchers investigated the earthquake induced damages to the sheet piles (Iai and Kameoka 1993). Here, the point of stock management is that the sheet-piling is so lower-cost than the ground improvement although the perfect control of uplift is not easy. Then, the damage assessment of soil-water-infra tri-system must be treated for discussing the efficient stock management and planning.

On the contrary, the efficiency of sheet-piling on mitigating structural damages associated with cracking and crushing of concrete and yielding of steel has been rarely studied. The reduced soil stiffness brought by large inelastic shear deformation and liquefaction leads to less damage to RC ducts inside the soil (JSCE 2002, Okhovat et al. 2009). In other words, we have to consider that the suppress of soil liquefaction by sheet pile installation as stated above may magnify the structural damage in contrast even though the uplift body motion could be fairly controlled. Damage mitigation related to constituent materials and rigid-body motion can be logically paradoxical. Thus, quantitative discussion is required in engineering practice as illustrated in **Figure 1**.

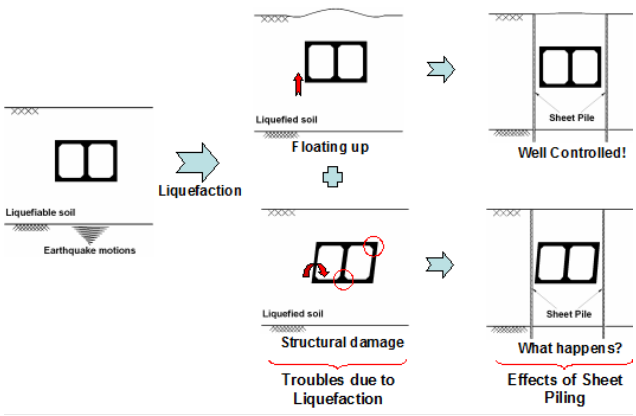

Figure 1. Schematic discussion: effect of sheet piling on the duct troubles in liquefiable soils.

In this paper, the effect of sheet piling on nonlinear seismic responses of underground RC ducts in liquefiable soils is investigated. First, the mechanism of sheet piles in alleviating uplift of underground RC is confirmed and computationally verified. Second, the effect of sheet piling on shear deformation and damage patterns of RC is aimed to be scrutinized. Finally, several properties of sheet piles are studied in consideration of performance based design schemes, and the effectiveness of sheet-piling is discussed as a whole.

2. NONLINEAR CONSTITUTIVE MODELS

2.1 Constitutive model for reinforced concrete (Maekawa et al. 2003)

A reinforced concrete material model has been constructed in the past decades by combining constitutive laws for cracked concrete and that for reinforcement (Foster *et al.* 2008). In this paper, the fixed multi-directional smeared crack constitutive models (Maekawa *et al*. 2003) are used to represent the relations of spatially averaged stresses and strains of RC elements. Crack spacing, its density in space and diameter of reinforcing bars are taken into account in both smeared and joint interface elements. The constitutive equations satisfy uniqueness for compression, tension and shear of cracked concrete. The bond performance between concrete and reinforcing bars is taken into account in terms of tension stiffening, and the space-averaged stress-strain relation of reinforcement is assumed so that it can represent the localized plasticity of steel. The hysteresis rule of reinforcement is formulated based upon Kato's model (1979) for a bare bar under reversed cyclic loads.

This RC constitutive modeling has been verified by a wide range of member-based and structural-oriented experiments. Generally speaking, the experiments directly used for constructing

constitutive models may not fully cover the stress and strain paths actually created in structural members. Thus, the mechanical constitutive models have to be further checked with the behavioral test results on the upper level of control volumes. Maekawa et al. (2003) used various mock-up structural experiments with both static and dynamic loading paths to verify the applicability and accuracy of the proposed fixed crack approach. By comparing series of shear tests of high strength concrete beams with the numerical finite element simulation (Tsuchiya et al. 2002), it was found that the shear behaviors of normal and high strength concrete members are fairly predictable as well. Irawan and Maekawa (1997) also used the model to simulate the RC shells like RC roofs of underground LNG tanks to check the structural safety under overburden soil pressures. They concluded that both material and geometrical nonlinearity need to be simultaneously taken into account in order that analysis results show close agreement with the reality. Herein, details of the RC modeling are all lined up in Maekawa et al. (2003).

2.2 Constitutive model for soil

A nonlinear path-dependent constitutive model of soil, which may predict the inelasticity of layered soils under earthquake excitation, is essential for a behavioral simulation of entire RC–soil systems properly. Here, the multi-spring modeling, which was originally presented by Towhata and Ishihara (1985), is applied to formulate the 3D shear stress-strain relation of the soil skeleton, and computationally reduced to the multi-yield plasticity functions (Okhovat *et al.* 2009) with Masing's rule (1926) for the shear hysteresis.

First, the total stress applied on soil particle assembly denoted by σ_{ij} can be decomposed of deviatoric shear stress (s_{ij}) and the effective mean stress (p) as,

$$\sigma_{ij} = s_{ij} + p\delta_{ij} \tag{1}$$

where δ_{ij} is Kronecker's delta symbol.

Soil is idealized as an assembly of finite numbers of inelastic components which are conceptually assembled in parallel (Towhara and Ishihara, 1985), to estimate the deviatoric shear stress. As each component is given different yield strength, all components are plasticized at different magnitudes of total shear strains, which results in a gradual internal yielding. Thus, the inelasticity appears naturally as a combined response of all components. Hence, the total shear stress carried by soil particles is expressed with regard to an integral of each component stress as,

$$s_{ij} = \sum_{m=1}^{n} s_{ij}^{m}(\varepsilon_{kl}, \varepsilon_{pkl}^{m}, G_0^{m}, F^{m}(p)) \tag{2}$$

where G_o^m, F^m and ε_{pkl}^m are the initial shear stiffness, the yield strength associated with the effective mean stress and the plastic strain tensor (k,l) of the *m-th* component, respectively. The path-dependency of the soil skeleton is represented by ε_{pkl}^m. These component parameters can be uniquely decided from the shear stress-strain relation (Maki *et al*. 2005). Furthermore, each yield strength denoted by F^m in Eq. (2) is changed according to the updated magnitude of confinement so that the total shear strength may follow the Mohr-Coulomb's frictional rule (Okhovat *et al.* 2009).

In order to determine the volumetric nonlinearity of soil skeleton, the authors simply divide the dilatancy into two components according to the microscopic events of soil particles. One is the consolidation (negative dilation) as an unrecoverable plasticity denoted by ε_{vc}. The other is the positive dilatancy associated with alternate shear stress due to

the overriding of soil particles which is recoverably denoted by ε_{vd} as,

$$p = 3K_0(\varepsilon_0 - \varepsilon_v), \quad \varepsilon_v = \varepsilon_{vc} + \varepsilon_{vd\,ij} \qquad (3)$$

where K_0 is the elastic volumetric bulk stiffness of soil particles assembly. The material parameters and functions used in this study are explained in the reference (Okhovat *et al.* 2009) in details.

Within this scheme, the liquefaction induced nonlinearity and cyclic dilatancy evolution can be consistently computed. **Figure 2** shows the computed pure shear stress-strain relation and the corresponding effective mean stress of the soil skeleton for different relative densities under the perfect undrained state. The total confinement stress applied to the soil skeleton and the pore water is kept constant. The pore water media is assumed to be perfect elastic body with no shear stiffness, and Biot's two-phase theory (1962) was coupled with the effective stress model of the soil skeleton as stated above.

Early liquefaction can be seen for loose sand, but the reduction of shear stiffness is suppressed for densely compacted sand in both cases of the experiment (**Figure 2a**; Towhata 2008) and the analysis (**Figure 2b**) even though the large shear stress amplitude is assumed. **Figure 2c** shows the sensitivity analysis in terms of the relative density to represent the magnitude of consolidation. Numbers of cycles (N) are required to have the reduction of shear stiffness accompanying the pore pressure rise. **Figure 2d** shows both experimental and analytically estimated strengths against liquefaction in terms of cyclic numbers up to the strain of 5%.

For experimental verification of combined RC-soil, the mock-up experiments of RC box culverts surrounded by sand under reversed cyclic shear (JSCE 2002) were conducted. The objective of the experiment was to investigate the ductility of RC underground ducts designed to withstand high shear deformation of dry soil foundations without liquefaction. Fairly good agreement was obtained between experiments and analyses of the load-displacement relations, shear deformational interaction and cracking patterns of concrete (Maekawa *et al*. 2003).

An *et al*. (1997) also used the model to clarify the collapse mechanism of two different sections of RC box culverts along a subway line which was damaged during the 1995 Hanshin-Awaji earthquake. It was thought that the earthquake intensity at the two sections would be the same because the distance between them is less than 10 *m*, but the mode of collapse significantly differs from each other. In fact, the one was located at the underground station and suffered from complete shear failure of the intermediate columns while the other of the tunnel nearby the collapsed stations had few diagonal cracks and no collapse was observed. The numerical simulation shows that the shear capacity and the ductility of underground RC ducts are critical factors in design for realizing higher seismic resistance (An *et al.* 1997).

2.3 Constitutive model for joint interface

Soil-structure interface properties between RC and foundation also have substantial influences on their interaction in general. As the soil and the structure generally have different stiffness characteristics, complete contact at the interface is not always assured. Under reversed cyclic shear, the sliding shear stress at the soil–structure interface takes place under strong seismic excitations, which brings about the local shear slip (Maekawa *et al*. 2003) and separation for the case of cohesive soils.

In this paper, the bi-linear model for the opening/closure mode is employed to model the interfacial kinematics. The normal stress is zero in case of separation, which means no stress is transferred through the joint when the interface is open. In contrast, the contact stiffness in closure mode is assigned a large value to ensure that no overlap is allowed, as shown in **Figure 3a**. For the sliding mode, the shear stress–strain relation is assumed to be linear, as shown in **Figure 3b**. The contact may slide if the magnitude of the applied shear stress exceeds the strength, which follows the Coulomb friction law (Maekawa et al. 2008). To apply this model, the initial condition of the interface must be simulated to represent the static earth pressure. This is achieved by performing an analysis that considers the body force of the soil mass alone before applying dynamic actions.

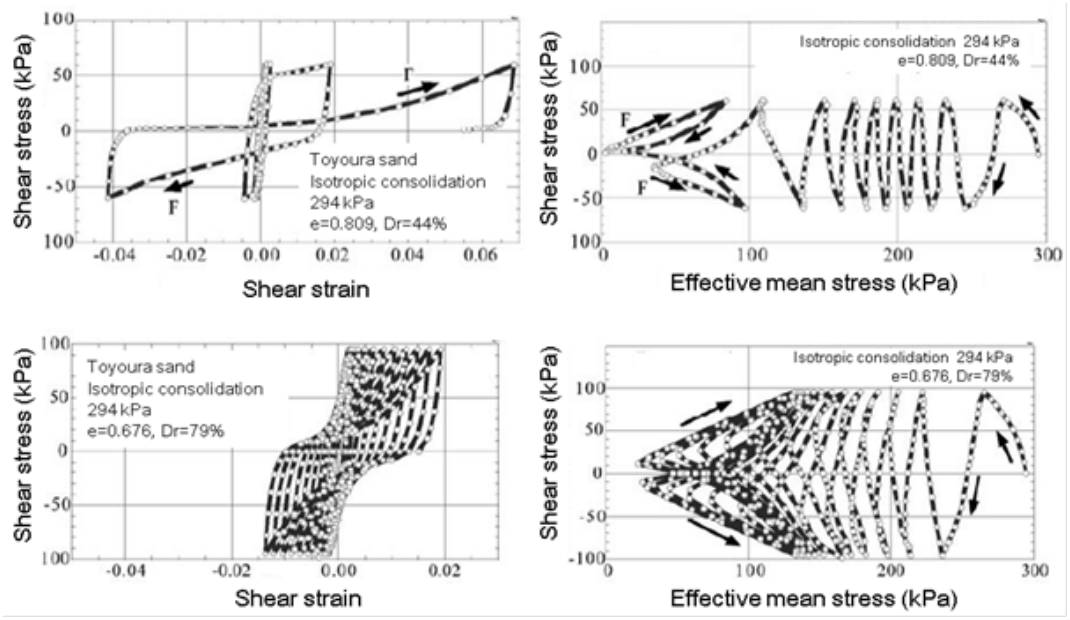

(a) Shear stress strain relation of Toyoura sand under undrained condition (Towhara 2008) Upper: loose sand D_r=44%, Lower: densely compacted sand

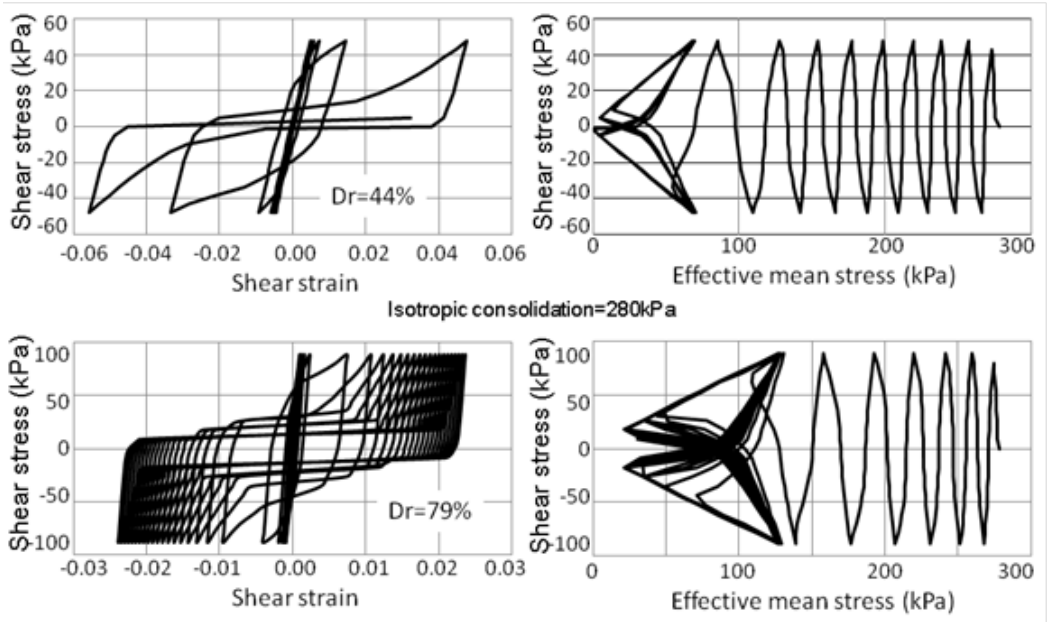

(b) Computed shear stress strain relation under undrained condition Upper: loose sand D_r=44%, Lower: densely compacted sand

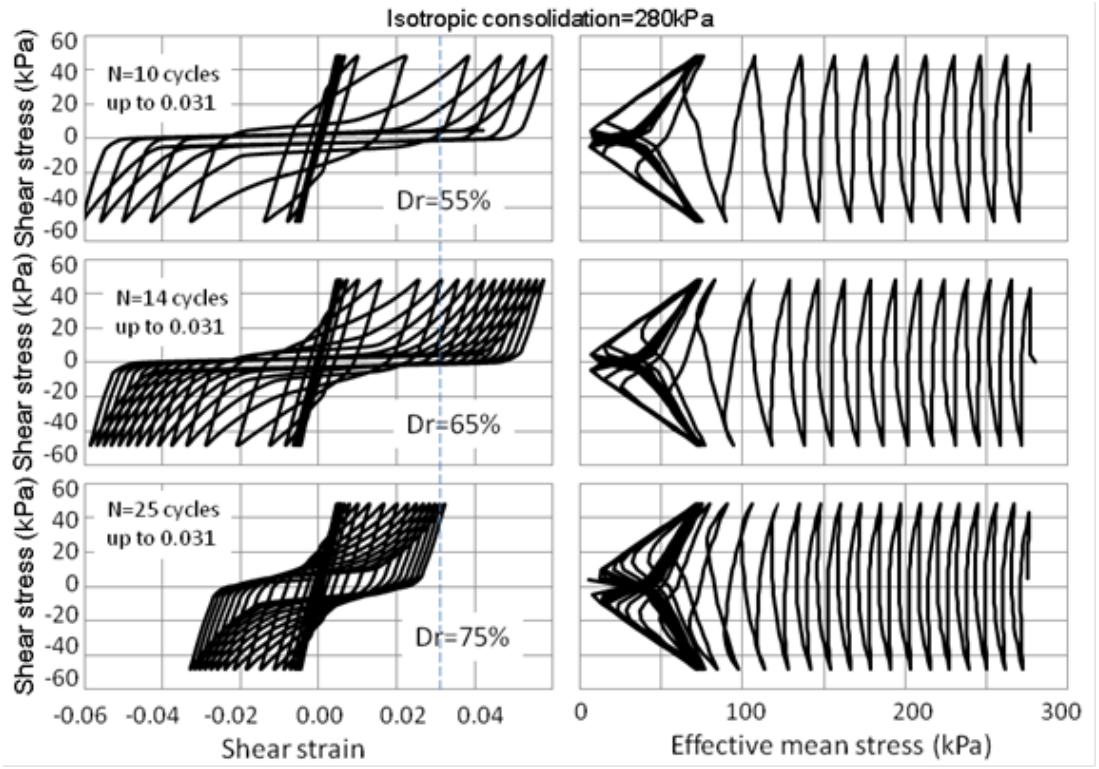

(c) Computed shear stress strain relation under undrained condition Sensitivity analysis in regard to the relative density: The same initial stiffness assumed.

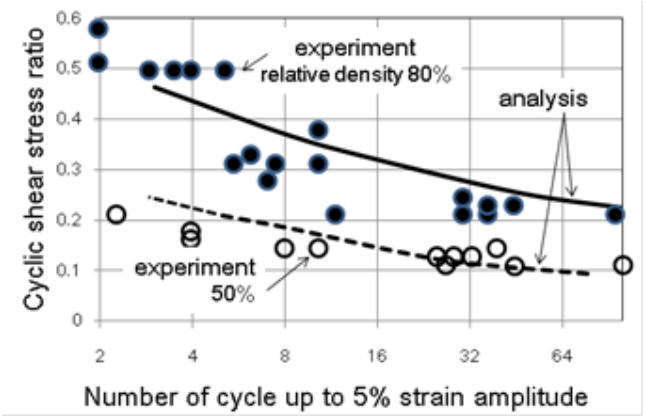

(d) Computed cyclic undrained triaxial strength in comparison with experiments (Toki at al. 1986)

Figure 2. Confinement dependent soil model under undrained cyclic shear loading.

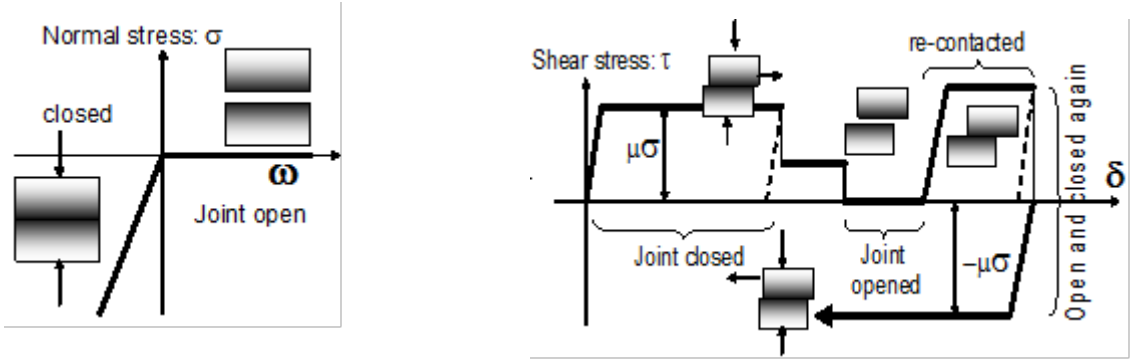

(a) Normal response (b) Shear response

Figure 3. Normal and shear response of linear elastic interface model (Maekawa et al. 2008)

The current joint interface model can be applied to the states of soil liquefaction as well as the drained static and dynamic conditions and pre-liquefied soils. Due to the dramatically reduced shear stiffness of liquefied soils, a quasi-hydrostatic pressure consequently develops inside the soil foundation after liquefaction, and it allows no separation to occur at the interfaces. Then, the joint interface modeling occupies minor roles on the structural damage analysis after liquefaction.

3. NUMERICAL MODELS

3.1 Model properties

To investigate the effect of sheet pile driving on RC ducts, a typical subway tunnel section is modeled whose wall and slab dimensions are shown in **Figure 4a**. The center column which mainly bears the dead weight of soil overlay has a rectangular cross section of 0.60 × 0.80 *m* and is idealized as firmly fixed to the slabs. The clear distance between two adjacent columns along the line is 3 *m*. The tunnel is stiffened with 45° haunches at every corner and has a longitudinal reinforcement ratio of 1.1% for side walls and slabs, 1.6% for the column, and web reinforcement ratio of 0.2% for all elements. The soil deposit is assumed not to be well compacted to numerically introduce the quick liquefaction. This liquefiable layer has a thickness of 15 *m* which is located on a 5-meter-thick layer of non-liquefiable hard soil which again lies on the bedrock as shown in **Figure 4a**.

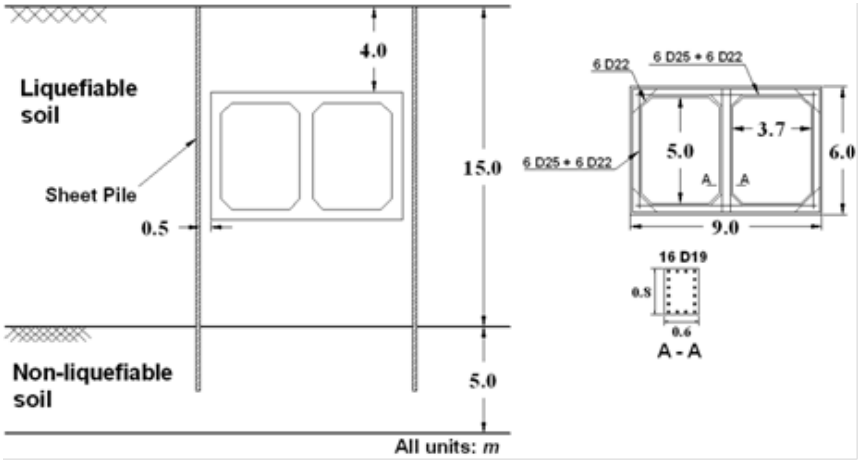

(a) Soil-structure layout

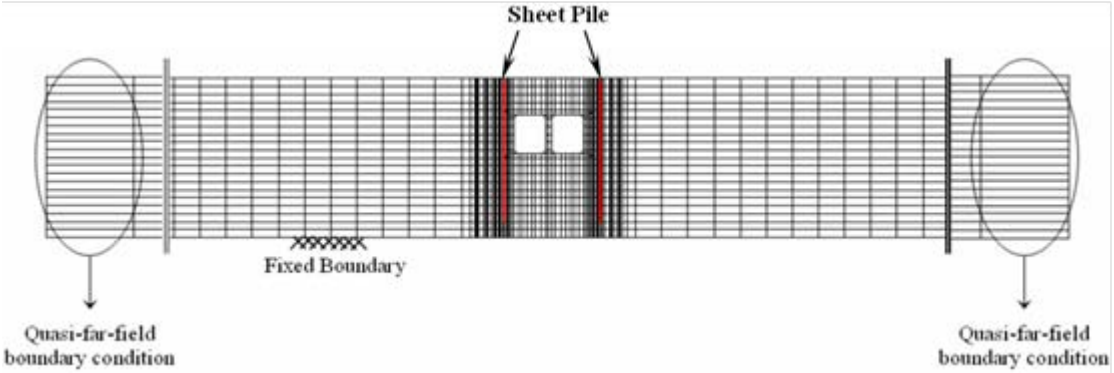

(b) Finite element mesh

Figure 4. Soil-structure system properties

Table 1. Material properties

Loose sandy layer		Non-liquefiable clayey layer	
Initial shear stiffness	35 MPa	Initial shear stiffness	105
Initial Poisson ratio	0.2	SPT *N*-value	15
Dry unit weight	14 kN/m^3	Dry unit weight	16
Friction angle	30 ^{o}	Friction angle	40 ^{o}
Relative density	32 %	Cohesion	100
		Relative Density	75 %
Reinforced concrete		**Interface**	
Compressive	24 MPa	Normal modulus (K_n)	10^8
Unit weight	24 kN/m^3	Shear modulus (K_s)	10^3
Poisson ratio	0.18	Friction angle	21^o
Steel young modulus	2.0x10^5 MPa	Cohesion	0
Steel yield stress	240 MPa		

The RC-soil interfacial elements are placed at junction planes between the foundation and RC elements. As the angle of internal friction of the model sand is 30°, the friction angle of the interface is obtained by using the formula tan-1[(2/3) tanϕ], which is about 21°; no cohesion between structure and ground is included. All the details of material properties for reinforcing bars, concrete, interface joint and soil layers are summarized in **Table 1**. In order to introduce quick liquefaction, the lower relative density is intentionally set forth as well.

The sheet pile is assumed to be made of steel with a Young modulus of 2.0 x 10^5 MPa and Poison's ratio of 0.3 by using elastic elements. For instance, the cross section and properties of a sheet pile used in practice are shown in **Figure 5**. The thickness of the steel finite elements is assumed (0.12 *m*) so that its bending stiffness would become equivalent to the real ones. No interface element is placed in between the sheet pile and the liquefiable soil elements since the localized gap would hardly take place owing to largely reduced shear stiffness of soil after liquefaction.

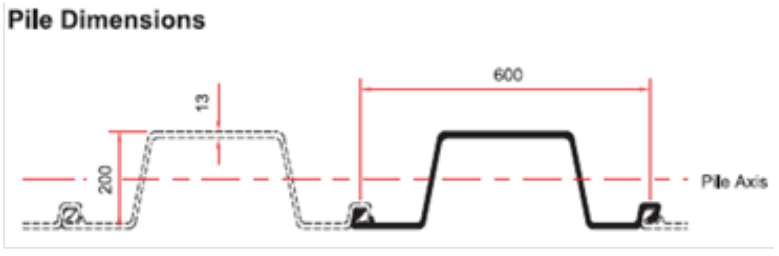

Unit in *mm*

Properties per 1 *m* of Wall			
Sectional Area	Mass	Moment of Inertia	Section Modulus
185.3 cm^2/m	145.0 kg/m	12090 cm^4/m	1175 cm^3/m

Figure 5. Cross section and properties of a sheet pile practically used.

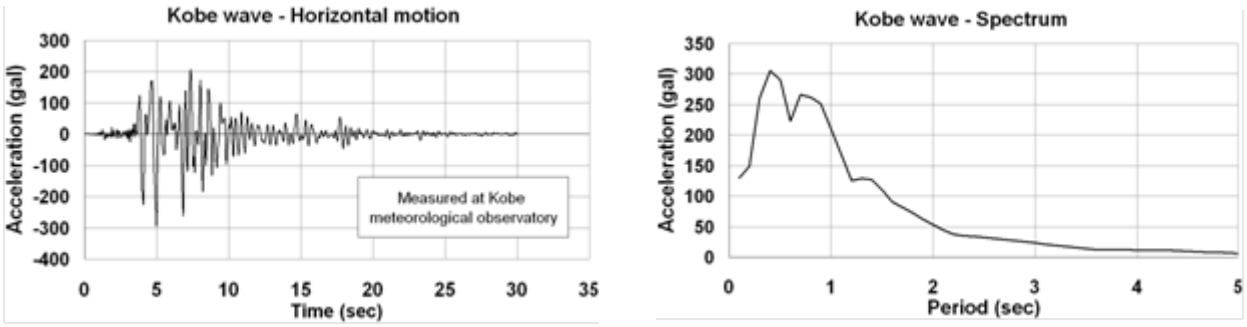

Figure 6. Input earthquake motion and its response spectrum.

By assuming the plane strain state, the finite element mesh used is composed of eight-node isoparametric 2D elements for the RC, soil and steel as it can be seen in **Figure 4b**. Totally, 7303 nodes and 2352 finite elements are arranged in the dynamic model. The north-south component of the rock base acceleration measured at 1995 Hanshin-Awaji earthquake, which is scale-adjusted to 0.3g based on the measurement at Kobe meteorological observatory, is used as the input bed rock motion in the seismic analysis. It shows the high horizontal ground acceleration with a short period as shown in **Figure 6**.

3.2 Boundary conditions

The boundary between the liquefiable soil deposit and the bedrock is assumed to be fixed and would act as the bottom boundary of the analysis domain at which the earthquake motion is imposed. The underground water level is assumed to be the ground surface so that the entire soil is saturated.

The soil deposit at the far fields should be assumed as the boundary of free vibration. In the shaking table tests of soil-structures, a laminar shear box may be used to simulate the quasi-far-field boundary. Here, quasi-far-field elements with a length of 10 *m* are placed at each extreme side of the analysis domain as illustrated in **Figure 4b**. Both stiffness and unit weight of far-field elements are increased 100 times fictitiously. It should be noted that the dynamic motion of these mock finite elements computationally coincides with that of free-vibration of the plane layered soils, but is not substantially affected by the motion of the target analysis domain including the structures. As the far-field mode of seismic motion is in laminated simple shear, the horizontal length of these boundaries is selected approximately half of the domain height so that the bending mode of deformation would not appear. In addition, confinement independent soil elements are used in the quasi-far-field zone in order to prevent the edge collapse in analysis. Consequently, this mock boundary simply makes the horizontal displacements at the right and left sides equal to each other, which is similar to the case of laminar shear boxes widely used in the shaking table tests.

Several trial analyses were carried out to determine the reasonable size of the analyzed domain so that the structural motion is converged. Finally, a relative large analyzed domain (200 *m*) was specified so as to make the wave reflection negligible.

3.3 Analysis procedure

The seismic analyses of the soil-structure system require an initial stress field in static equilibrium before the dynamic loads. Then, an initial static analysis under the drained state was firstly performed to determine the initial stress field and the

corresponding static earth pressure applied on the duct. This static stress field is then used as the initial condition for the subsequent dynamic run. In general, reproduced static soil stress fields might depend on the process of construction. But, it was confirmed by the preliminary analyses that the initial earth pressure on the RC ducts has minor influence on the damage of structures when high nonlinearity is induced to both soil and structure under large ground motions.

In order to investigate the effect of the sheet pile length and its anchorage into the non-liquefiable soil, three analyses are carried out with three different lengths of sheet piles which are assumed to be installed at 0.5 *m* away from the both sides of the tunnel as shown in **Figure 4a**. Since the thickness of the liquefiable soil is 15 *m* as mentioned before, these three sheet pile lengths (12 *m*, 15 *m* and 18 *m*) are respectively correspondent to a) the non-anchored case, b) just touching the non-liquefiable soil surface and c) anchored three-meter deep in the non-liquefiable soil. Furthermore, three more analyses were performed with the same sheet pile lengths but installed at 2.5 *m* away from both sides of the tunnel. Finally, the dimension of the sheet pile elements is changed to study the effect of sheet pile flexural stiffness.

It should be noted that the fully undrained state for soil is rather severe in view of liquefaction, but not so far from the reality. The required time for drainage from the sand layer of several-meter-thick is 10-30 min, which is adequately longer than the duration time of earthquake loading (Towhata 2008).

4. SHEET PILE-DUCT-SOIL INTERACTION

4.1 Effect of sheet piling

It has been concluded that the effect of sheet pile driving is very obvious in reducing the uplift of underground ducts when an earthquake induces liquefaction. Hamada *et al.* (2006) carried out some centrifuge model tests to show the effects of cutoff walls surrounding a buried structure for mitigation of its floating up, and concluded that the displacement of the structure with cutoff walls is directly influenced by the thickness of liquefied ground under the structure. By conducting some 1-G shaking table tests, Koseki *et al.* (1994) and Towhata (2008) showed that the floating of underground structures could be significantly reduced when sheet piles with drainage are employed as a method of uplift mitigation (**Figure 7**).

According to the finite element results in the present research, the uplift of the tunnel is significantly controlled when sheet piles with the length of 18 *m* are installed at 0.5 *m* away from both sides of the tunnel as shown in **Figure 8**. The deformed meshes after the earthquake motion for the cases with and without sheet piles are compared in **Figure 9**. It is clear that the floating of the ducts is accompanied by the inward movement of liquefied soil beneath the structure which can push it upward. The sheet piles can reduce or even prevent such a soil movement, and the uplift of the underground structure becomes much smaller.

Liu and Song (2006) discuss that cutoff walls cannot always inhibit excess pore water pressure in progress. In comparison with the case with no cutoff walls, the magnitude of excess pore pressure of the enclosed liquefiable soils depends on the soil properties and the seismicity. The excess pore pressure responses of the above-mentioned cases at the centerline of the tunnel are shown in **Figure 10a**. The excess pore pressures are expressed in terms of the ratio of excess pore pressure to the initial effective overburden pressure.

Although the excess pore pressure in both cases develops almost similarly at the beginning of the seismic motion, it would decrease while the uplift of the tunnel takes place. In fact, the flotation of the duct is accompanied by larger shear deformation of surrounding soil which contributes to the lowering of excess pore pressure due to the positive dilatancy. The sheet piles alleviate the floatation so that the excess pore pressure remains nearly constant. Furthermore, the excess pore pressure 1.5 *m* above the structure (with sheet piles) is smaller than that in the case of no sheet pile as shown in **Figure 10b**. But, it is clear that the soil may also be liquefied with sheet piles installed.

The mean shear deformation of the underground duct, on the other hand, increases when sheet piles are installed. The maximum mean shear deformation of the duct rises from 0.28 % in the case of no sheet pile to 0.37 % with sheet piles (**Figure 11**). This is attributed to the enlarged stiffness difference of the structure and the soil. In fact, its stiffness variation of the structure and the surrounding soil has the most significant influence on the distortion of the structure due to racking deformations (Wang 1993). Without sheet piles, the structure remains rather stiff relative to the soil medium and does not deform much.

However, by restricting shear deformation in the enclosed soil, sheet piles can recover the soil stiffness degradation. Consequently, more deformational demand would be conditioned to the seismic RC structural design. As a result, more damage would occur at the structural elements in the case of sheet pile installation as can be seen in **Figure 12**. The yielding zone steel reinforcement close to the edge of the members is enlarged due to the sheet-pile construction, and the concrete compressive strain is a little increased. It means that the risk of spalling of cover concrete and the unrecoverable crack width will be increased.

It can be concluded that although installation of sheet piles can drastically alleviate the uplift of underground structures, it may cause the structure to suffer from more damage. Thus, a rational design of sheet piling should consider both of its positive and negative effects in term of structural damage and rigid-body stability.

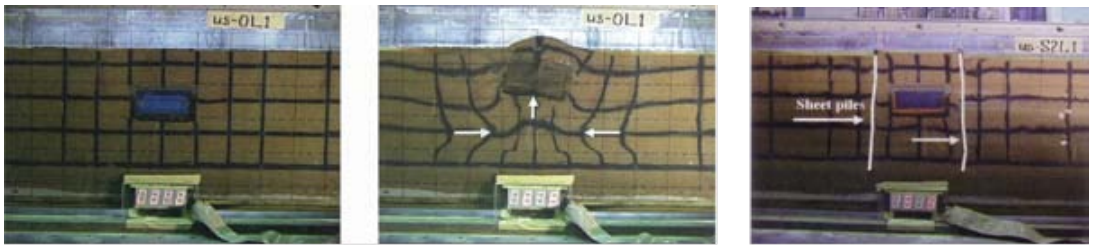

(a) Before test (b) Without mitigation (c) With sheet piles with drainage

Figure 7. Shaking model for floating of an embedded box by Towhata (2008)

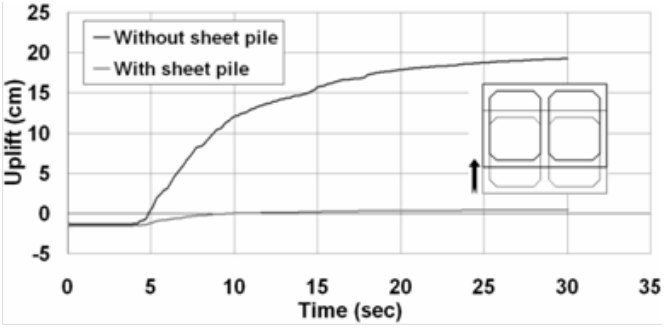

Figure 8. Effect of sheet pile in reducing uplift of the duct: simulation.

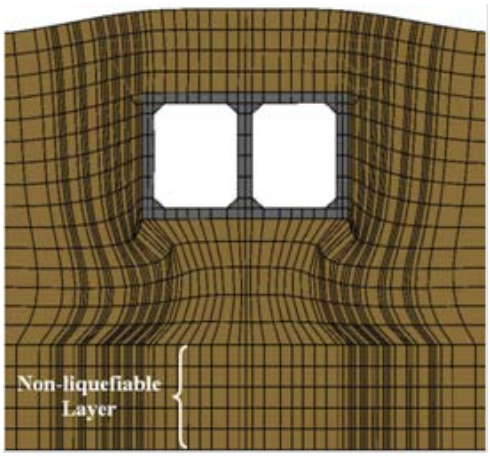

(a)

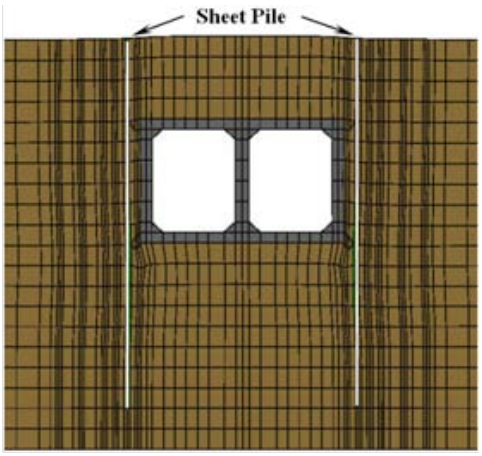

(b)

Figure 9. Part of the deformed mesh (enlarged 5 times) (a) without sheet pile (b) with sheet pile.

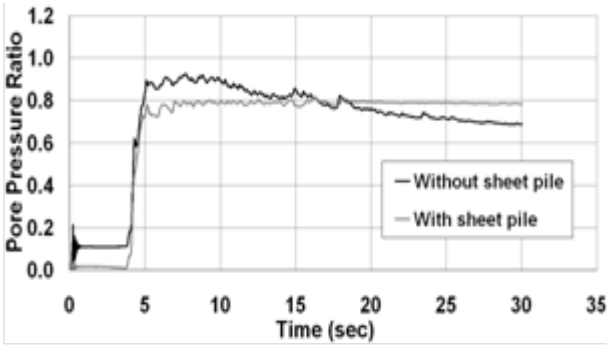

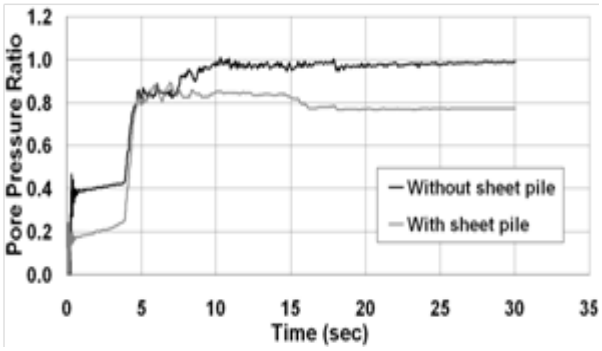

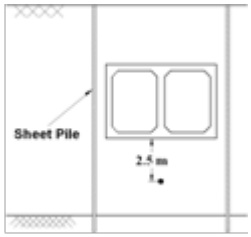

(a) 2.5 m below the tunnel

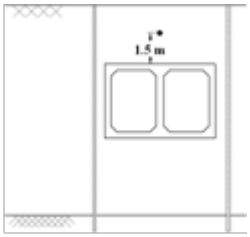

(b) 1.5 m above the tunnel

Figure 10. Excessive pore pressures in soil foundation.

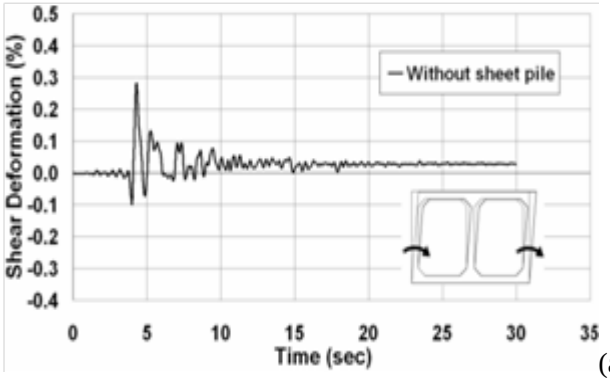

(a)

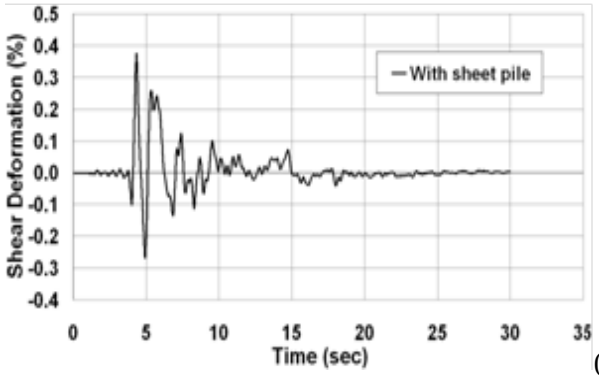

(b)

Figure 11. Shear deformation response of the tunnel (a) without sheet pile (b) with sheet pile

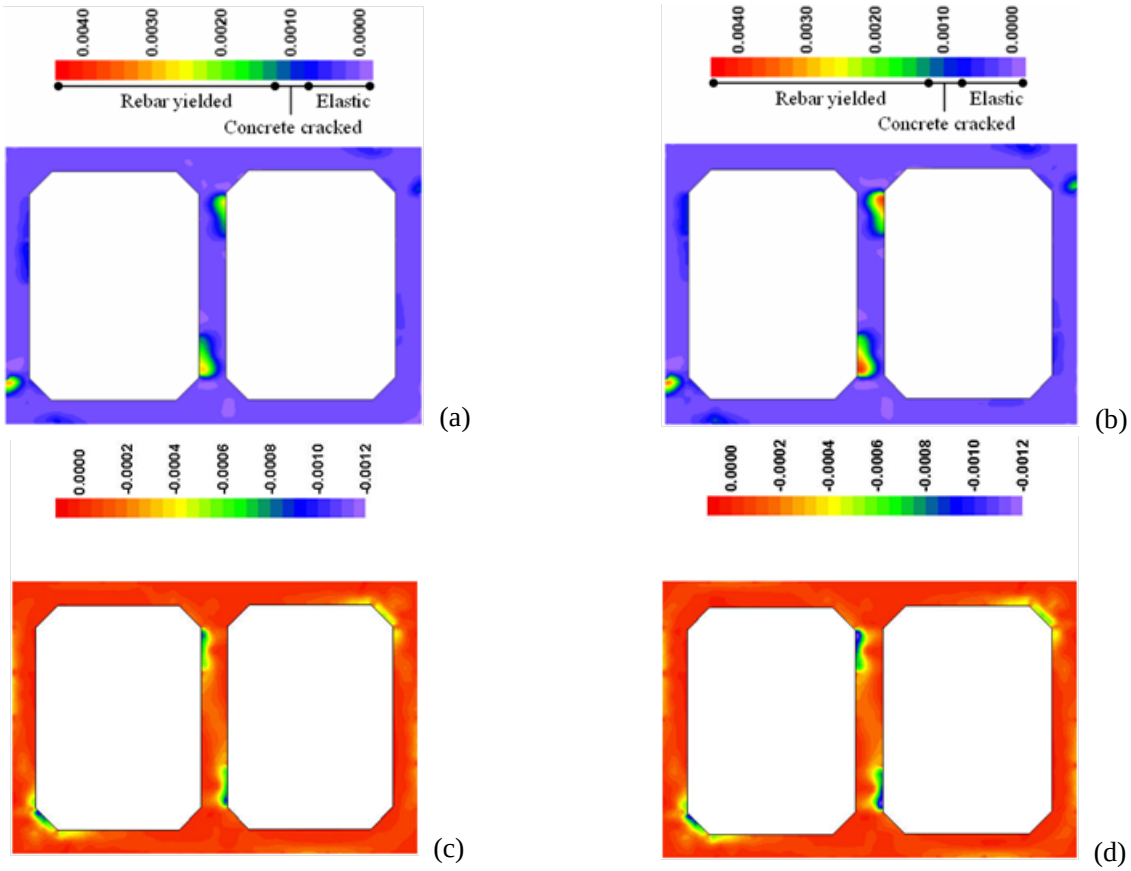

Figure 12. Strain state of the tunnel at the maximum shear deformation (a) principal tensile strain without sheet pile (b) principal tensile strain with sheet pile(c) principal compressive strain without sheet pile (d) principal compressive strain with sheet pile

4.2 Effect of sheet pile length

Although sheet piling has been a proved current technology, its design procedure needs to follow the consideration of cost performance in practice. The length of the sheet piles which is one of the important parameters regarding those issues should be rationally decided. As a sensitivity analysis, two lengths of the sheet piles (L) are discussed (15 and 12 *m*).

Figure 13 shows the uplift of the duct. By comparing **Figure 13** and **Figure 8**, it can be understood that in the case of L=15 *m*, where the tip of sheet pile just touches the non-liquefiable soil surface without being driven into that layer, the uplift motion of the tunnel is significantly reduced as well. In fact, the maximum uplift of the structure after the seismic motion would decrease from 20.8 *cm* (no sheet pile) to 1.9 *cm* or 2.4 *cm* with the sheet pile length of 18 *m* or 15 *m*, respectively. It can be observed in **Figure 14a** that sheet piles prevent the main mechanism of the uplift of underground ducts, i.e., flow of the liquefied soil and squeeze beneath the ducts (Koseki *et al.* 1997 and Hashash *et al.* 2001) even if it is not anchored inside the non-liquefiable soil. Thus, it seems unnecessary for the sheet piles to be driven deep into the non-liquefiable layer which usually needs much more energy.

On the other hand, if the sheet piles do not penetrate enough inside the soil layers, their performance against the uplift would be dramatically declined. The ultimate uplift of the tunnel would decrease to just 9.8 *cm* when the length of the sheet pile is 12 *m* (**Figure 13**), i.e. 3 *m* of the liquefiable

soil layer is not blocked under the sheet piles and the inward soil movement can still squeeze the subway to uplift as it can be observed in **Figure 14b**.

The effect of the sheet piles' length on the shear deformation of the RC duct is shown in **Figure 15**. It can be seen that when the sheet piles do not penetrate into the non-liquefiable soil, the shear deformation response of the structure does not change so much in comparison with the case where the sheet piles are driven 3 *m* into non-liquefiable soil (**Figure 11b**). Furthermore, the shear strain of the duct section slightly reduces when L = 12 *m* due to the decreased gap of the stiffness of the soil and the structure as previously discussed. However, the sheet piles with insufficient penetration length may not effectively control the uplift of the underground structure.

All the results are summarized in **Figure 16** which shows the effect of sheet pile length on controlling the uplift and shear deformation of the RC duct. Here, the attention is focused on the ratio of sheet pile length to the liquefiable soil depth (λ), which is associated with the constructability as,

$$\lambda = \frac{L_p}{D_l} \tag{7}$$

where L_p is the length of driven sheet pile and D_l is the liquefiable soil depth.

It is obvious that the desirable effect of sheet pile in alleviating the uplift of ducts is much more than its negative effect in increasing the structural shear deformation - and thus - damage to RC ducts. In addition, it can be concluded that the performance of the sheet piles when they are not anchored inside the non-liquefiable soil layers but penetrate enough into the liquefiable soil is more or less similar to the case where they are deeply driven into the non-liquefiable and usually stiff soil layers. However, it should be pointed out that the border of soil layers with different properties is not very clear in reality.

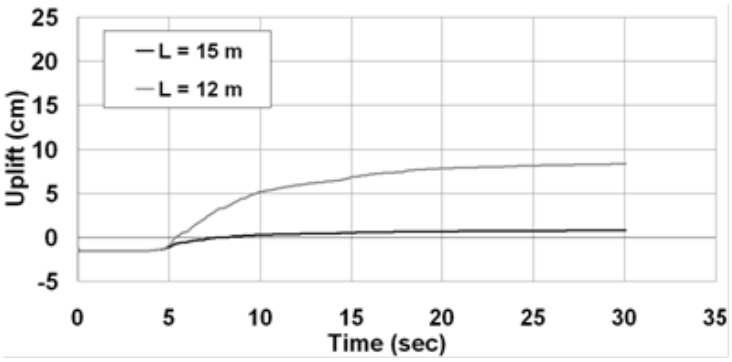

Figure 13. Effect of sheet pile length in reducing uplift

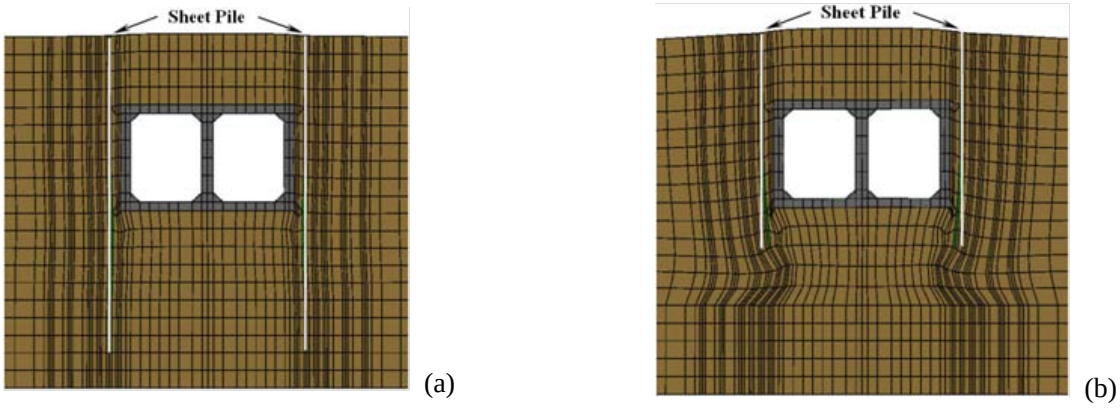

(a) (b)

Figure 14. Part of the deformed mesh (enlarged 5 times) with sheet piles when (a) L=15 *m* (b) L=12 *m*

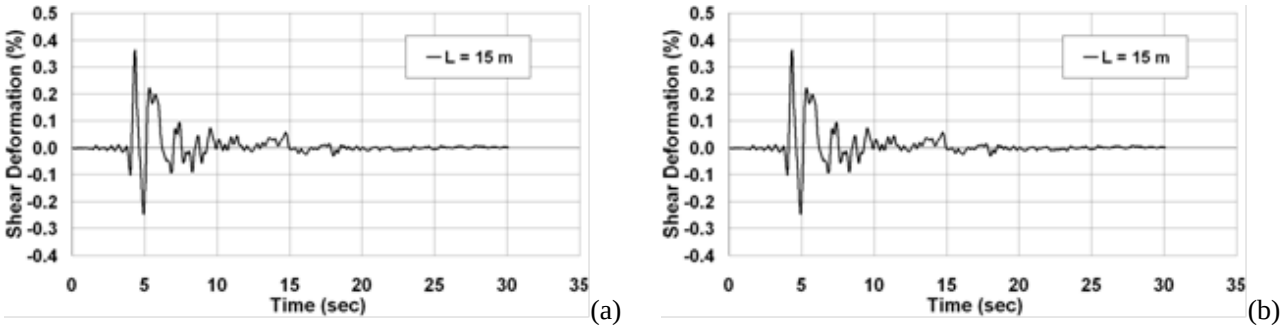

Figure 15. Shear strain response of the tunnel (a) L = 15 m (b) L = 12 m

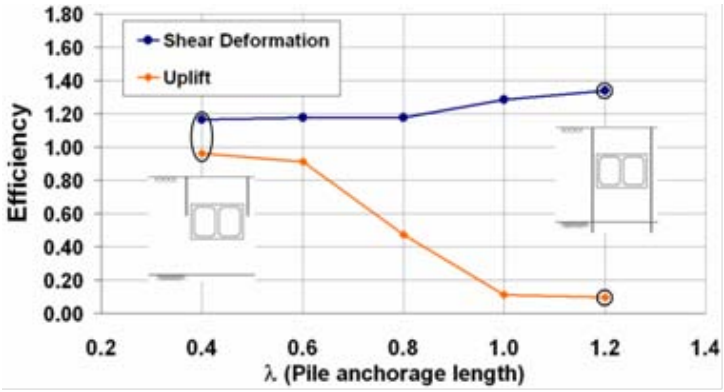

Figure 16. Effect of sheet pile length on the uplift and shear deformation of tunnel

4.3 Effect of sheet pile lateral location

Many researchers have argued that the installation of sheet piles must be as close to the protected underground structure as possible in order to be effective in reduction of the uplift (Kimura *et al.* 1995; Liu and Song 2006). Furthermore, sheet piling quite close to the old or newly built underground structure is rather possible nowadays owing to current technology development. In order to investigate the effect of the lateral spacing between sheet piles and the duct, three cases are analyzed with the similar assumptions of previous models except that the distance (denoted by D) of the sheet piles away from the RC duct is increased from 0.5 *m* to 2.5 *m*.

Figure 17 shows the uplift response of the duct section with three different sheet pile lengths of 12 *m*, 15 *m*, and 18 *m* when D is kept 2.5 *m*. In comparison with previous results in which D is 0.5 *m* (**Figure 8** and **Figure 13**), it is detected that with an increase in the distance of the sheet piles from the duct, the uplift significantly increases. This can be explained by the fact that although the sheet piles prevent the flow of the liquefied soils around the structure, the local deformation of the liquefied soils in between the sheet piles proceeds, and the RC duct is still pushed upward.

The shear deformation response of the underground RC when sheet piles are installed at 2.5 *m* away from the duct is shown in **Figure 18**. By comparing with the shear deformation of the RC when D is 0.5 *m* (**Figure 11** and **Figure 15**), it can be understood that although the shear deformation is slightly reduced by installing the sheet piles at further distances from the duct, it is still larger than that of the case with no sheet pile. Thus, it is not recommended to install sheet piles at further distances from the underground structures in order to decrease their shear deformation.

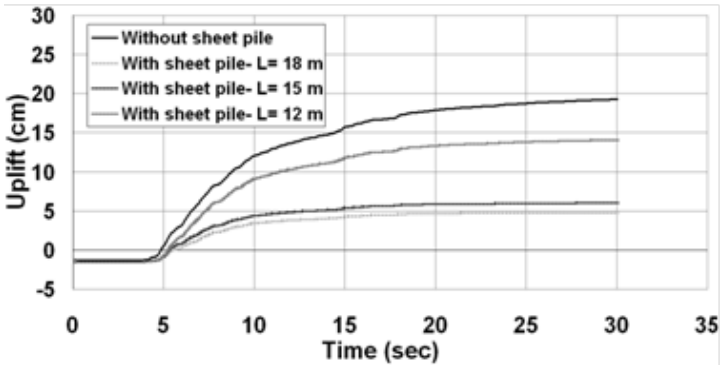

Figure 17. Uplift response of the tunnel when D = 2.5 m

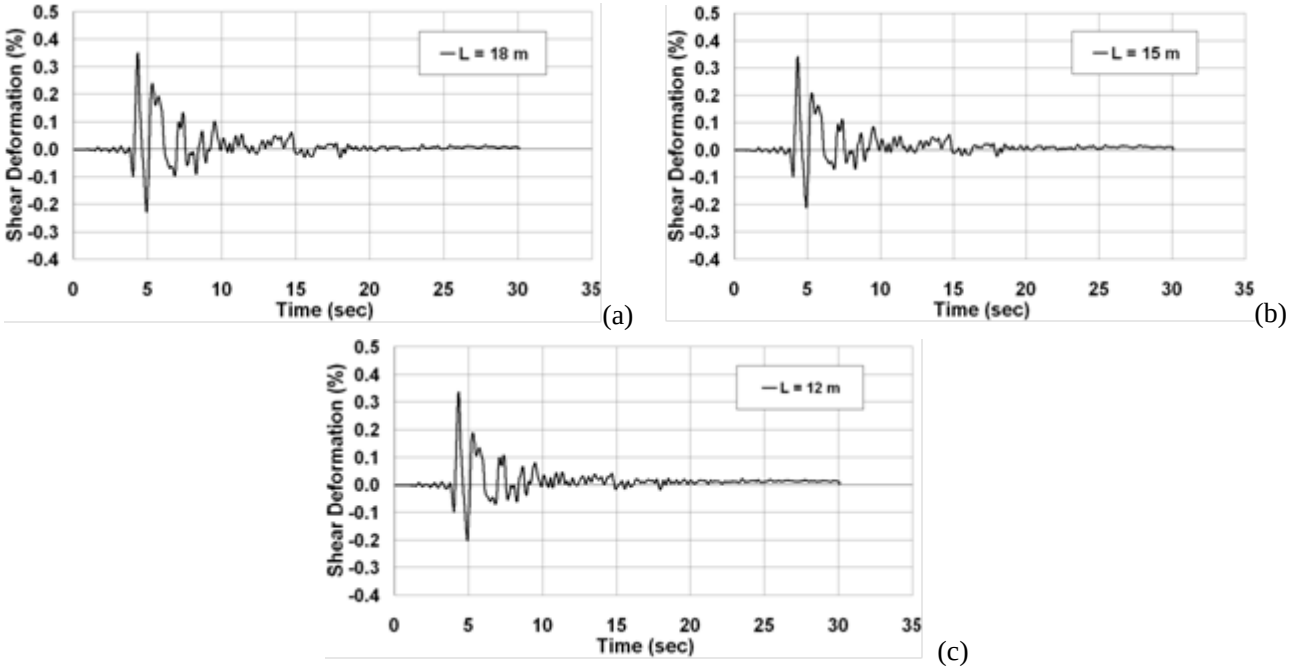

Figure 18. Shear strain response of the tunnel when D = 2.5 *m* (a) L = 18 *m* (b) L = 15 *m* (c) L = 12 *m*

4.4 Effect of sheet pile stiffness

It is known that the increase in sheet pile stiffness would reduce the uplift of ducts (Kimura *et al.* 1995). But on the contrary, the increased stiffness of the sheet pile may elevate the induced force to the underground structure accompanying larger shear deformations of the RC ducts. In order to study the effect of sheet pile stiffness on the RC ducts, the thickness of the sheet piles (L=18 *m* and D=0.5 *m*) is computationally reduced from 12 *cm* to 8 *cm* so that its bending rigidity would be considerably degenerated. The uplift and shear deformation responses of the tunnel are shown in **Figure 19** and **Figure 20**, respectively. As can be seen in these figures, the structural damage of RC would relatively decrease although the uplift motion of the underground structure does not increase so much. The maximum shear deformation of the underground RC duct is reduced from 0.37 % in the stiffer sheet pile case (**Figure 11b**) to 0.33 % in the case with thinner sheet piles. Hence, it is quite reasonable at the design stage to minimize the required stiffness of the sheet piles regarding the soil pressure and deformation in order to have less underground structural damage.

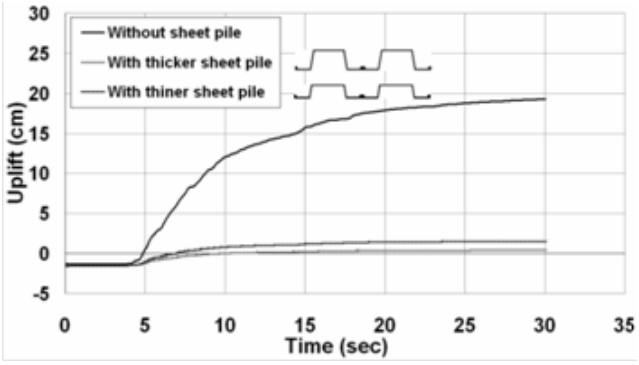

Figure 19. Uplift response of the tunnel with thinner sheet pile.

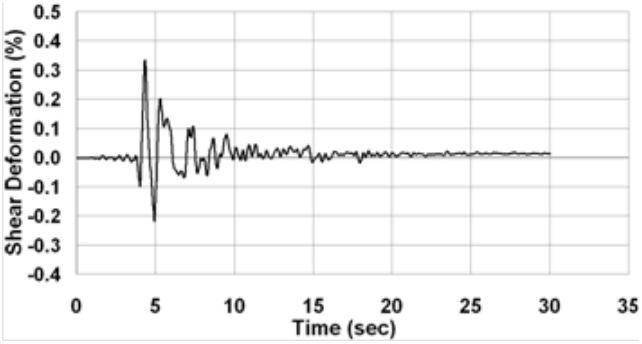

Figure 20. Shear strain response of the duct with thinner sheet pile.

5. CONCLUSIONS

The effects of sheet piling on the nonlinear seismic responses of underground RC ducts in saturated liquefiable soils were discussed as a tool of infra-stock management. A parametric study on the sheet pile location, penetration depth and the bending stiffness was carried out to examine damage control parameters, and the following conclusions are earned.

1. Although installation of sheet piles can drastically alleviate the uplift of underground RC ducts, it may cause the structure to suffer more damage due to the remained shear stiffness of the soil surrounded by the sheet piles. Hence, a rational design of sheet piling should consider both of its positive and negative effects on the underground RC ducts.
2. In order to minimize the damages in use of the sheet piling, the flexural stiffness of the sheet piles is one of controllable factors in practice and the sensitivity of the stiffness on the structural damage to RC was clarified. Increase in the lateral spacing of the sheet piles from the structure has almost nothing to do with the structural damages. But, it is sensitive to the uplift in motion. Thus, the close installation of sheet piles is beneficial in view of the entire damage control of underground RC.
3. Even if sheet piles are not anchored into non-liquefiable soil layers but they deeply penetrate inside the liquefiable soil, the overall performance of sheet piles, i.e., both structural damage control and uplift mitigation, is thought to be acceptable in practice. As this effectiveness depends on the site situations, the performance shall be examined in combination with the soil and RC structural nonlinearity.

Then, it is proposed in line with the urban stock management that the sheet piling, which is much lower cost rather than the ground improvement or structural strengthening, can be an efficient measure to reduce the collapse risk of existing underground RC infrastructures if the small rigid body motion is allowed, for example, aqua-ducts to maintain water channels, the electric transmission and telecommunication cables.

ACKNOWLEDMENTS

The authors appreciate Mr. A. Kitamura and Dr. Tagaya of Giken Seisakusho Co. Ltd and Dr. K. Nagai and Dr. Uchimura of the University of Tokyo for their discussion on the pile driving technology and seismic strengthening of existing infrastructure.

REFERENCES

An, X., Shawky, A. A. and Maekawa, K. (1997). The collapse mechanism of a subway station during the

Great Hanshin earthquake, *Cement and Concrete Composite*, 19, 241-257.

Foster, S., Vecchio, F. and Maekawa, K. (Eds) (2008). Practitoners' guide to finite element modeling of reinforced structures, Bulletin 45, federation internationale du beton, 2008.

Hall, W. J. and O'Rourke, T. D. (1991). Seismic behavior and vulnerability of pipelines, *Proc. Third US Conf. Lifeline Earthquake Engineering*, 761-773.

Hamada, N., Goto, S., Mano, H. and Ohnishi, Y. (2006). Protection effects of buried structures from soil liquefaction hazard by means of cutoff walls, *J. of Japan Society of Civil Engineers*, 62(1), 12-21, *(in Japanese)*.

Hashash, Y. M. A., Hook, J. J., Schmidt, B., Yao, J. (2001). Seismic design and analysis of underground structures, *Tunnelling and Underground Space Technology*, 16, 247-293.

Iai, S., Kameoka, T. (1993). Finite element analysis of earthquake induced damage to anchored sheet pile quay walls, *Soils and Foundations*, 33(1), 71-91.

Irawan, P. and Maekawa, K. (1997). Path-dependent nonlinear analysis of reinforced concrete shell, *J. Mater. Conc. Struct. Pavements*, JSCE, 557/V-34, 121-34.

Ishihara, K., Alex, Acacio, A. and Towhata, I. (1993). Liquefaction-induced ground damage in Dagupan in the July 16, 1990 Luzon earthquake, *Soils and Foundations*, 33(1), 133-154.

Japan Society of Civil Engineers (2002). Recommended code and manual for seismic performance verification of out-door important structures of nuclear power plants, *Concrete International Library*.

Kato, B. (1979). Mechanical properties of steel under load cycles idealizing seismic action, *CEB Bulletin D'Information*, 131, 7-27.

Kimura, T., Takemura, J., Hiro-oka, A. and Okamura, M. (1995). Countermeasures against liquefaction of sand deposits with structures, *Proc. First International Conference on Earthquake Geotechnical Engineering*, 1203-1224, Tokyo, Japan.

Koseki, J., Koga, Y., Takahashi, A. (1994). Model shaking tests and finite element analysis on uplift of common utility ducts during earthquakes, *Proc. of 9th Japan Earthquake Engineering Symposium*, 997-1002 (*in Japanese*).

Koseki, J., Matsuo, O., Koga, Y. (1997). Uplift behavior of underground structures caused by liquefaction of surrounding soil during earthquake, *Soils and Foundations*, 37(1), 97-108.

Koseki, J., Matsuo, O. and Tanaka, S. (1998). Uplift of sewer pipes caused by earthquake-induced liquefaction of surrounding soil, *Soils and Foundations*, 38(3), 75-87.

Liu, H., Song, E. (2006). Working mechanism of cutoff walls in reducing uplift of large underground structures induced by soil liquefaction, *Computers Geotechnics*, 33, 209-221.

Maekawa, K., Irawan, P. and Okamura, H. (1997). Path-dependent three-dimensional constitutive laws of reinforced concrete: Formulation and experimental verifications, *Structural Engineering and Mechanics*, 5(6), 743-54.

Maekawa, K. and An, X. (2000). Shear failure and ductility of RC columns after yielding of main reinforcement, *Engineering Fracture Mechanics*, 65, 335-368.

Maekawa, K., Pimanmas, A. and Okamura, H. (2003). *Nonlinear Mechanics of Reinforced Concrete*, Spon Press, London.

Maekawa, K., Fukuura, N. and Soltani, M. (2008). Path-dependent high cycle fatigue modeling of joint interfaces in structural concrete, *Journal of Advanced Concrete Technology*, 6(1), 227-242.

Maki, T., Maekawa, K. and Mutsuyoshi, H. (2005). RC pile-soil interaction analysis using a 3D-finite

element method with fiber theory-based beam elements, *Earthquake Engineering and Structural Dynamics*, 99, 1-26.

Masing, G. (1926). Eigenspannungen and Verfestigung Beim Messing, *Proc. of Second International Congress of Applied Mechanics*, 332, Zurich.

Okhovat, M. R., Shang, F. and Maekawa, K. (2009). Nonlinear seismic response and damage of reinforced concrete ducts in liquefiable soils, *Journal of Advanced Concrete Technology*, 7(3).

Toki, S., Tatsuoka, F., Miura, S., Yoshimi, Y., Yasuda, S. and Makihara, Y. (1986). Cyclic undrained triaxial strength of sand by cooperative test program, *Soils and Foundations*, 26(3), 117-128.

Towhata, I. (2008). "*Geotechnical Earthquake Engineering*," Springer, Germany.

Towhata, I. and Ishihara, K. (1985). Modeling soil behaviors under principal stress axes rotation, *5th Int. Conf. on Numerical Method in Geomechanics*, Nagoya, 523-530.

Tsuchiya, S., Mishima, T. and Maekawa, K. (2002). Shear failure and numerical performance evaluation of RC beam members with high-strength materials, *J. Mater. Conc. Struct. Pavements*, JSCE, 697/V-54, 65-84.

Wang, J. N. (1993). Seismic design of tunnels: a state-of-the-art approach, Monograph, monograph 7, Parsons, Brinckerhoff, Quade and Douglas Inc, New York.

Wang, W. L., Wang, T. T., Su, J. J., Lin, C. H., Seng, C. R. and Huang, T. H. (2001). Assessment of damage in mountain tunnels due to the Taiwan Chi-Chi earthquake, *Tunneling Underground Space Technology*, 16(3), 133-150.

Zheng, J., Suzuki, K., Ohbo, N. and Prevost, J. H. (1996). Evaluation of sheet pile-ring countermeasure against liquefaction for oil tank site, *Soil Dynamics and Earthquake Engineering*, 15, 369-379.